



Identification of *ortho*-hydroxy anilide as a novel scaffold for lysine demethylase 5 inhibitors

Pattaporn Jaikhan^a, Benjaporn Buranrat^{a,b}, Yukihiro Itoh^a, Jiranan Chotitumnavee^a, Takashi Kurohara^a, Takayoshi Suzuki^{a,c,*}

^a Graduate School of Medical Science, Kyoto Prefectural University of Medicine, 1-5 Shimogamohangi-cho, Sakyo-ku, Kyoto 606-0823, Japan

^b Biomedical Sciences Research Unit, Faculty of Medicine, Mahasarakham University, Muang District, Maha Sarakham 44000, Thailand

^c CREST, Japan Science and Technology Agency (JST), 4-1-8 Honcho, Kawaguchi, Saitama 332-0012, Japan

ARTICLE INFO

Keywords:

Small molecule
Drug design
Histone deacetylase
Lysine demethylase
Inhibitor

ABSTRACT

Fe(II)/ α -ketoglutarate-dependent lysine demethylases (KDMs) are attractive drug targets for several diseases including cancer. In this study, we designed and screened *ortho*-substituted anilides that are expected to function as Fe(II) chelators, and identified *ortho*-hydroxy anilide as a novel scaffold for KDM5A inhibitors. Treatment of human lung cancer A549 cells with a prodrug form of 4-carboxy-2-hydroxy-formanilide (**9c**) increased trimethylated lysine 4 on histone H3 level, suggesting KDM5 inhibition in the cells.

Epigenetics refers to a post-translational process with heritable mechanisms regardless of changes in the DNA sequence. Recent studies have uncovered diverse relationships between epigenetic regulation, such as histone modification, and pathological stage in oncogenesis/neurological disorders.^{1–3} Among the epigenetic mechanisms, histone lysine methylation at various sites of histone proteins has been extensively studied.⁴ The lysine methylation is mediated by two major types of enzymes, lysine methyl transferases (KMTs) and lysine demethylases (KDMs).⁴ KDMs are further divided into two classes on the basis of their structures and catalytic mechanisms to oxidize methyl groups bound to the ϵ -amino group (N^ϵ) of lysine. One class is composed of flavin-dependent oxidases, namely, lysine-specific demethylase 1 (LSD1: also called KDM1A)⁵ and LSD2 (KDM1B).⁶ The other class is a family of Fe(II)/ α -ketoglutarate (α KG)-dependent oxidases (KDM2–8) sharing a conserved catalytic domain, jumonji C (JmjC) domain.⁷

Much effort has been devoted to understanding the roles of KDMs in biological process as well as pathological development and progression.⁸ The deregulation of KDMs has been reported in various types of human cancers and neurological disorders.^{3,9,10} In addition, the pharmacological inhibition of KDMs is expected to be a novel therapeutic strategy for these diseases. The KDM4 subfamily proteins, for instance, are up-regulated in esophageal carcinoma¹¹ and breast cancer,¹² and the inhibition of expression or the enzymatic inhibition of KDM4 induces a decrease in the proliferation of several cancers.^{2,13,14} KDM5 proteins, which are often up-regulated in lung, breast, and prostate cancers, promote tumor progression and drug resistance.^{15,16} It has

been reported that KDM5 inhibitors reduce the survival of drug-tolerant cancer cells.¹⁷ KDM6 is associated with several physiological functions including cellular stress, and various inflammatory responses.^{18,19,20} KDM6 inhibitors decrease the production of cytokines, such as pro-inflammatory tumor necrosis factor, and KDM6 inhibition may be a promising approach for the treatment of inflammatory diseases.^{21,22,23} Thus, KDM inhibitors are of interest as therapeutic agents for several diseases as well as chemical probes for KDMs.

To date, a number of structurally diverse compounds have been reported as KDM inhibitors.^{24,25} However, only KDM1 inhibitors that target flavin-dependent oxidases have reached the clinical trial phase.²⁶ Inhibitors targeting Fe(II)/ α KG-dependent KDMs are still in the rudimentary stage. As studies of crystal structures have revealed the presence of conserved Fe(II) and α KG binding sites in the KDM catalytic pocket, various α KG mimics, which consist of an iron-chelator and carboxylate, have been widely used as α KG-competitive inhibitors. *N*-oxalyl glycine (NOG, **1**), a broad-spectrum KDM inhibitor, is one example of an α KG mimetic KDM inhibitor (Fig. 1).²⁷ In addition, some pyridine, 8-hydroxyquinoline, and hydroxamate derivatives representing other iron-chelating inhibitors have been reported as KDM inhibitors. 2,4-PDCA (**2**),²⁸ IOX1 (**3**),²⁹ GSK-J1 (**4**),³⁰ and NCDM-81a (**5**)³¹ are representative examples (Fig. 1). However, these inhibitors have low cellular activity because of their low cell membrane permeability, which is due to the high polarity of the iron-chelating motif conjugated with a carboxylate group, even though their ester prodrug forms are used. Therefore, α KG mimics having sufficiently low polarity

* Corresponding author.

E-mail address: suzukit@koto.kpu-m.ac.jp (T. Suzuki).

<https://doi.org/10.1016/j.bmcl.2019.03.028>

Received 6 February 2019; Received in revised form 13 March 2019; Accepted 20 March 2019

Available online 21 March 2019

0960-894X/© 2019 Elsevier Ltd. All rights reserved.

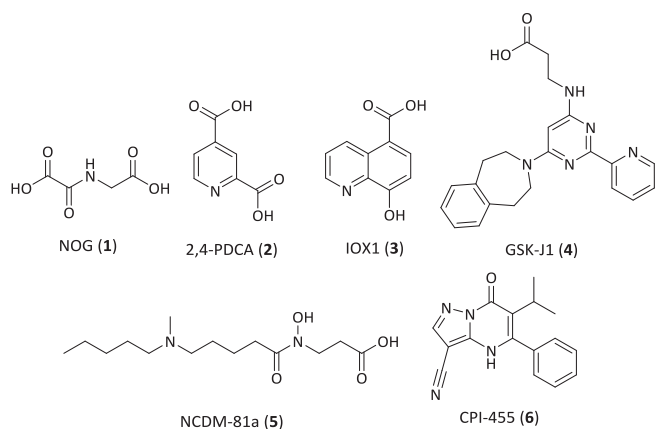


Fig. 1. Structures of representative KDM inhibitors.

are required as cell-active KDM inhibitors. Although CPI-455 (6, Fig. 1),¹⁷ a novel KDM inhibitor, exhibited relatively high activity in a cellular assay, the number of cell-active α KG mimic inhibitors remains limited. In this study, we attempted to identify a novel α KG mimic scaffold for Fe(II)/ α KG-dependent KDM inhibitors.

We focused on an *ortho*-substituted anilide structure. Various *ortho*-amino anilides have been reported as histone deacetylase (HDAC) inhibitors, such as MS-275 (7) and T247 (8) (Fig. 2A).³² The *ortho*-amino anilide moiety of these inhibitors can chelate a zinc ion in the HDAC catalytic site, inhibiting HDACs strongly. Based on the metal chelating mechanism of the *ortho*-amino anilide group of HDAC inhibitors, we thought that *ortho*-substituted anilide would be used as a novel pharmacophore of KDM inhibitors. In other words, we expected that the *ortho*-substituted anilide scaffold would be useful as an iron chelator, and that *ortho*-substituted anilides bearing a carboxylate group would work as an α KG competitor (Fig. 2B). Before we experimentally verified our hypotheses, we explored the possibility that an *ortho*-substituted anilide would work as an iron chelator by performing a theoretical quantum calculation study with Gaussian 09.³³ We estimated the complex formation energies between an *ortho*-substituted anilide and a zinc ion or an iron ion, and compared them (Fig. 3). To simplify the calculations, we used water molecules as the metal ligand (Fig. 3). Because the zinc ion in HDACs and the iron ion in KDMs are pentavalent and hexavalent, respectively,^{34,35,36} we optimized the structures of a pentavalent zinc complex and a hexavalent iron complex. The geometry optimization and the vibration frequency of the *ortho*-substituted anilide and its complexes with the metals were calculated using a density functional model (B3LYP) with the 6–31+G* basis set. As a result, the Gibbs free energies (ΔG) for the formation of amino anilide- Zn^{2+} , amino anilide- Fe^{2+} , and hydroxy anilide- Fe^{2+} complexes were estimated to be -31.94 kcal/mol, -30.12 kcal/mol, and -26.46 kcal/mol, respectively, and there was little difference between them. These calculation results strongly suggested that the *ortho*-substituted anilides should coordinate not only with Zn^{2+} but also with Fe^{2+} . Therefore, we attempted to evaluate *ortho*-substituted anilides as novel KDM

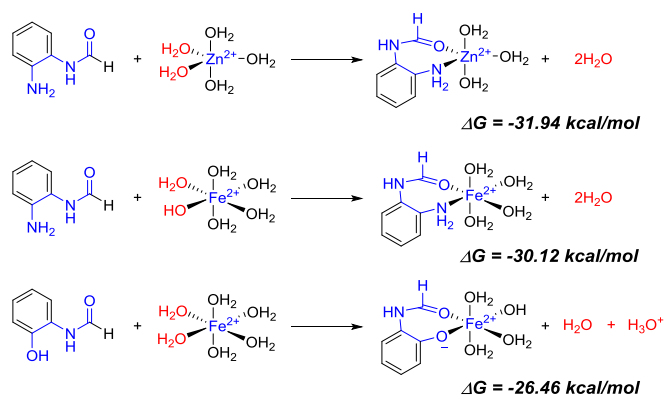


Fig. 3. Estimation of Gibbs free energies (ΔG) in complex formation between *ortho*-amino anilide and zinc/iron ion by a theoretical quantum calculation study with Gaussian 09.

inhibitors. *Ortho*-substituted anilides 9 and 10 were designed: acetamide and formamide substitutions represent two different species of the anilide core, and a hydroxy group was also used as an *ortho*-substituted group as well as an amino group (Fig. 2B).

The designed *ortho*-anilides were synthesized from corresponding benzoic acids, as outlined in Scheme 1. Esterification of compounds 11, 13, and 15 afforded methyl esters 12, 14, and 16, respectively. Compounds 12, 14, and 16 were treated with acetyl chloride to yield compounds 19, 21, and 22, respectively. Compound 19 was converted into amine 20 by hydrogenation in the presence of Pd/C. Finally, deprotection of compounds 20–22 under the basic condition gave desired compounds 9a, 9b, and 10a, respectively. On the other hand, compounds 9c and 10b were prepared by the direct formamidation of compounds 17 and 18, respectively. The final compounds were purified by chromatography and their purities (> 95%) were confirmed by HPLC analysis.

The activities of the *ortho*-substituted anilides were initially screened against KDM5A (also known as JARID1A) enzyme in the AlphaScreen™ assay. NCDM-81a (5), a KDM5A inhibitor, was used as positive control. Although amino-substituted acetanilide 9a did not inhibit KDM5A at 50 μM , hydroxy-substituted acetanilide 9b showed weak inhibitory activity against KDM5A at the same concentration (Fig. 4), suggesting that the hydroxy group is preferred to the amino group in KDM5A inhibition. Then, we tested hydroxy-substituted acetanilides 10 bearing a 4-carboxylate group. The KDM5A inhibitory activity of 10b was significantly higher than that of 10a, which indicates that the formanilide moiety is better than the acetanilide moiety. Accordingly, we tested hydroxy-substituted formanilide 9c bearing a 3-carboxylate group, and found that 9c exhibited pronounced KDM5A inhibitory activity. These results suggest that the 3-carboxylates, if anything, are preferred to the 4-carboxylates in the KDM5A inhibition by the *ortho*-hydroxy anilides. A superimposition of a stable conformation of an *ortho*-hydroxy anilide coordinating Fe^{2+} ion with the conformation of α KG bound to KDM5A indicates that the 3-position

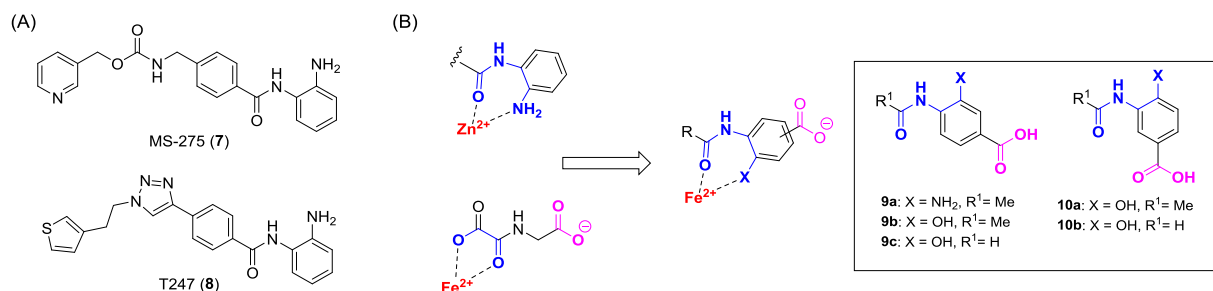
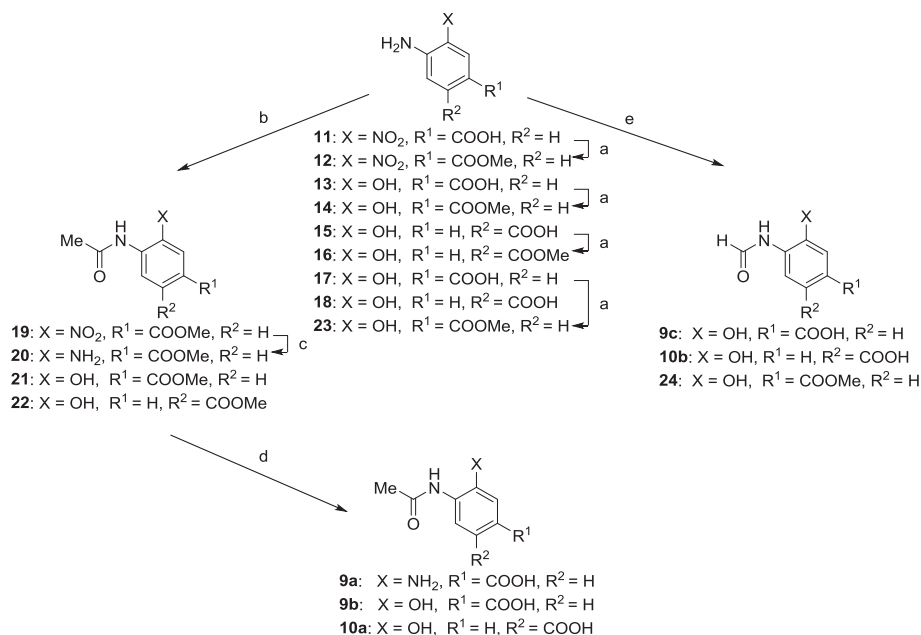


Fig. 2. (A) Structures of representative *ortho*-amino anilide HDAC inhibitors, MS-275 (7) and T247 (8). (B) Design of *ortho*-substituted anilides for KDM inhibitors.



Scheme 1. Synthesis of compounds **9** and **10**.^a (a) Reagents and conditions: (a) conc. H₂SO₄, MeOH, reflux, 24 h, 68–100%; (b) acetyl chloride, Et₃N, THF, 40 °C, 24 h, 41–62%; (c) Pd/C, H₂, MeOH, RT, 5 h, 98%; (d) NaOH, MeOH, H₂O, 60 °C, 3–24 h, 40–81%; (e) formic acid, H₂O, 70 °C, 24 h, 83–90%.)

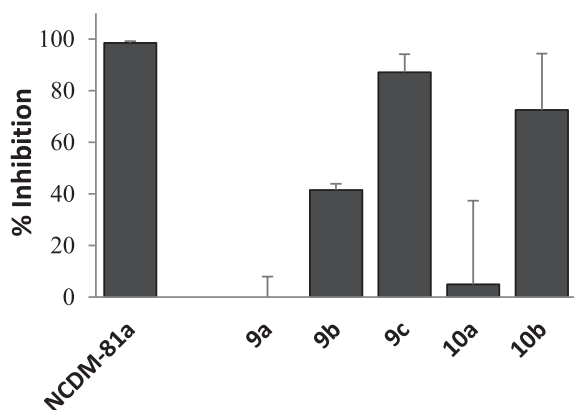


Fig. 4. AlphaScreen™ assay of KDM5A inhibitory activities of compounds **5**, **9**, and **10**. The % inhibition in the presence of 3 μM NCDM-81a (**5**) or 50 μM compounds **9** and **10**.

is located at the closer proximity to the carboxylate of αKG (Supplementary Fig. S1). This may be one of the reasons that the 3-carboxylates inhibit KDM5A more strongly than 4-carboxylates. Furthermore, we determined the IC₅₀ values of compounds **9c** and **10b** for KDM5A inhibition. As shown in Table 1, the IC₅₀ values of **9c** and **10b** for KDM5A were 46 μM and 48 μM, respectively. Based on these results, we selected compound **9c** for further evaluation. To investigate KDM subfamily protein selectivity of compound **9c**, KDM4A and KDM6B inhibition assays were performed. As shown in Table 1, compound **9c** at 50 μM demonstrated only 20% and 38% inhibition of KDM4A and KDM6B, respectively. Moreover, we evaluated HDAC-inhibitory activity of compound **9c** because it might work as a zinc ion chelator for HDAC inhibition. As shown in Table 1, compound **9c** did not strongly inhibit HDAC1 at 100 μM. Thus, compound **9c** inhibition against KDM5A was stronger than those against KDM4A, KDM6B, and HDAC1 enzymes.

Subsequently, we investigated whether compound **9c** inhibits KDM5A in a competitive binding manner with αKG by the formaldehyde dehydrogenase (FDH)-coupled demethylation assay.³⁷ As shown in Fig. 5, the KDM5A inhibitory activity of compound **9c**

Table 1
Inhibitory activities of compounds.

| Compound | IC ₅₀ /%Inhibition | | | |
|-----------------------|-------------------------------|---------------------------------|------------------|------------------|
| | KDM4A | KDM5A | KDM6B | HDAC1 |
| 9c | 20% ^a | 46 ± 11 μM 87% ^a | 38% ^a | 6% ^c |
| 10b | ND ^b | 48 ± 3.6 μM 73% ^a | ND ^b | ND ^b |
| NOG (1) | 85 ± 1.9 μM | ND ^b | ND ^b | ND ^b |
| NCDM-81a (5) | ND ^b | 79 ± 0.1 nM | ND ^b | ND ^b |
| GSK-J1 (4) | ND ^b | ND ^b | 16 ± 4.3 nM | ND ^b |
| SAHA | ND ^b | ND ^b | ND ^b | 95% ^d |

^a % inhibition at 50 μM.

^b ND = no data available.

^c % inhibition at 100 μM.

^d % inhibition at 10 μM: SAHA was used as a positive control for HDAC1 assay.

(200 μM) decreased from 97% to 44% as the concentration of αKG increased from 50 to 1000 μM. These results suggested that the KDM5A inhibitory effect of compound **9c** may result from the binding of **9c** to the αKG binding site of KDM5A.

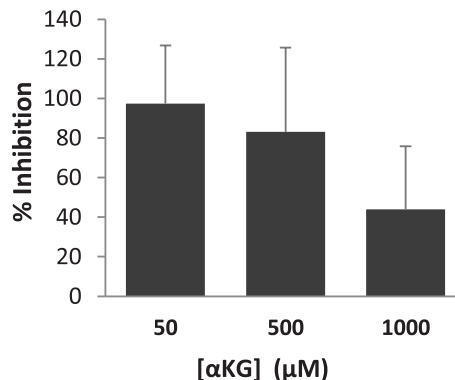


Fig. 5. % inhibition of compound **9c** (200 μM) in the presence of various concentrations of αKG in the FDH-coupled demethylation assay.

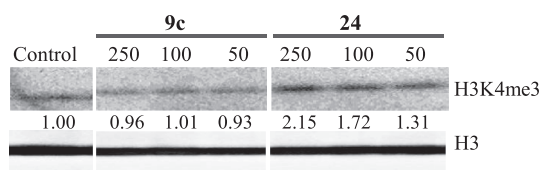


Fig. 6. Western blot detection of methylated histone level in A549 cells treated with **9c** and **24**. H3K4me3 levels after 24 h incubation with **9c** and **24**. Values of the H3K4me3/H3 ratio determined by optical density measurement of the blots are shown.

Next, we investigated the effects of compound **9c** on histone methylation levels in human lung cancer cell line A549 where KDM5A is overexpressed.^{38,39,40} After treating A549 cells with compound **9c** for 24 h, whole proteins were extracted and the levels of trimethylated lysine 4 on histone H3 (H3K4me3), which is a substrate of KDM5A, were determined by western blot analysis. As shown in Fig. 6, compound **9c** did not affect H3K4me3 levels. This may be due to the high polarity of **9c**, which lowers its cell membrane permeability. We also tested compound **24**, which is the methyl ester prodrug of compound **9c**. Prodrug compound **24** was synthesized by the esterification of compound **17**, followed by formamidation (Scheme 1). Unlike compound **9c**, compound **24** increased H3K4me3 levels in a dose-dependent manner (Fig. 6). An analysis of the H3K4me3/H3 ratio by plotting the optical density values revealed that compound **24** increased the ratio by approximately 1.7–2.2 times at 100–250 μM. A previous report suggested that the methyl ester prodrug of hydroxamate-based inhibitor NCDM-81a (**5**) increased the ratio by approximately 1.6 times at 300 μM.³¹ Therefore, the cellular activity of a prodrug of *ortho*-hydroxy anilide was better than that of a hydroxamate-based inhibitor. We also investigated the effect of compounds **9c** and **24** on cell viability, however, neither of them showed significant cytotoxicity against A549 cells at 250 μM (data not shown). Further structural optimization is underway for the identification of *ortho*-substituted anilides which exhibit anti-cancer activity.

In conclusion, based on an *ortho*-substituted anilide as a zinc chelator of HDAC inhibitors, we designed and synthesized *ortho*-substituted anilides as iron chelators for JmjC-domain-containing KDM inhibitors. We identified *ortho*-hydroxy anilide as a novel scaffold for KDM5A inhibitors. Compound **9c** showed moderate inhibitory activity against KDM5A with an IC₅₀ of 46 μM, and inhibited KDM5A stronger than two other JmjC-domain-containing family members, KDM4A and KDM6B. In cell-based assays, compound **24**, a prodrug of compound **9c**, increased H3K4me3 levels in human lung cancer cell line A549. The discovery of the *ortho*-hydroxy anilide scaffold for KDM5 inhibitors will be useful for the new design of biological tools for probing the biological functions of KDM5 and therapeutic agents, such as anticancer drugs acting on KDM5. Further structural modification of this anilide scaffold is underway.

Acknowledgments

The authors would like to thank Yasunao Hattori, Kenichi Akaji, Naoya Ieda, Mitsuyasu Kawaguchi, and Hidehiko Nakagawa for

technical support. This work was supported in part by the JST CREST program (T.S.; JPMJCR14L2).

Appendix A. Supplementary data

Supplementary data to this article can be found online at <https://doi.org/10.1016/j.bmcl.2019.03.028>.

References

- Pedersen MT, Helin K. *Trends Cell Biol.* 2010;20:662.
- McGrath J, Trojer P. *Pharmacol Ther.* 2015;150:1.
- Park SY, Park JW, Chun YS. *Pharmacol Res.* 2016;105:146.
- Kubicek S, Jenuwein T. *Cell.* 2004;119:903.
- Shi Y, Lan F, Matson C, et al. *Cell.* 2004;119:941.
- Karytinos A, Forneris F, Profumo A, et al. *J Biol Chem.* 2009;284:17775.
- Klose RJ, Kallin EM, Zhang Y. *Nat Rev Genet.* 2006;7:715.
- Chakravarty S, Jhelum P, Bhat UA, et al. *Biochim Biophys Acta, Mol Cell Biol Lipids.* 2017;1863:152.
- Peter CJ, Akbarian S. *Trends Mol Med.* 2011;17:372.
- Flavahan WA, Gaskell E, Bernstein BE. *Science.* 2017;357.
- Cloos PA, Christensen J, Agger K. *Nature.* 2006;442:307.
- Ye Q, Holowatyj A, Wu J, et al. *Am J Cancer Res.* 2015;5:1519.
- Luo X, Liu Y, Kubicek S, et al. *J Am Chem Soc.* 2011;133:9451.
- Jin C, Yang L, Xie M, et al. *Proc Natl Acad Sci USA.* 2014;111:9235.
- Hayami S, Yoshimatsu M, Veerakumarasivam A, et al. *Mol Cancer.* 2010;13:59.[].
- Stein J, Majores M, Rohde M, et al. *Am J Pathol.* 2014;184:2430.
- Vinogradova M, Gehling VS, Gustafson A, et al. *Nat Chem Biol.* 2016;12:531.
- Lan F, Bayliss PE, Rinn JL, et al. *Nature.* 2007;449:689.
- Lee HY, Choi K, Oh H, Park YK, Park H. *Mol Cells.* 2014;37:43.
- Neidhart M, Gay RE, Gay S. *Arthritis Rheum.* 2000;43:1719.
- Cribbs A, Hookway ES, Wells G, et al. *J Biol Chem.* 2018;293:2422.
- Hu J, Wang X, Chen L, et al. *Bioorg Med Chem Lett.* 2016;26:721.
- Jia W, Wu W, Yang D, et al. *FASEB J.* 2018;32:4031.
- Thinnes CC, England KS, Kawamura A, et al. *Biochim Biophys Acta.* 2014;1839–11416.
- Hauser AT, Robaa D, Jung M. *Curr Opin Chem Biol.* 2018;45:73.
- M Licheva, A Neudolt, IM Bennani-Baiti, Cancer Epigenetics Drug Database (CEDD)-Clinical data, v1.1.1. Cancer Epigenetics Society (https://ces.b2sg.org/cedd/clinical_kdmi/), 2016.
- Rose NR, Woon EC, Kingham GL, et al. *J Med Chem.* 1810;2010:53.
- Rose NR, Ng SS, Mecinović J, et al. *J Med Chem.* 2008;51:7053–7056.
- Hokpinkson RJ, Tumber A, Yapp C, et al. *Chem Sci.* 2013;4:3110.
- Kruidenier L, Chung CW, Cheng Z, et al. *Nature.* 2012;488:404.
- Itoh Y, Sawada H, Suzuki M, et al. *ACS Med Chem Lett.* 2015;6:665.
- Suzuki T, Kasuya Y, Itoh Y, et al. *PLoS One.* 2013;8:e68669.
- Frisch MJ, Trucks GW, Schlegel HB, Scuseria GE, Robb MA, Cheeseman JR, Scalmani G, Barone V, Petersson GA, Nakatsuji H, Li X, Caricato M, Marenich A, Bloino J, Janesko BG, Gomperts R, Mennucci B, Hratchian HP, Ortiz JV, Izmaylov AF, Sonnenberg JL, Williams-Young D, Ding F, Lipparini F, Egidi F, Goings J, Peng B, Petrone A, Henderson T, Ranasinghe D, Zakrzewski VG, Gao J, Rega N, Zheng G, Liang W, Hada M, Ehara M, Toyota K, Fukuda R, Hasegawa J, Ishida M, Nakajima T, Honda Y, Kitao O, Nakai H, Vreven T, Throssell K, Montgomery Jr JA, Peralta JE, Ogliaro F, Bearpark M, Heyd JJ, Brothers E, Kudin KN, Staroverov VN, Keith T, Kobayashi R, Normand J, Raghavachari K, Rendell A, Burant JC, Iyengar SS, Tomasi J, Cossi M, Millam JM, Klene M, Adamo C, Cammi R, Ochterski JW, Martin RL, Morokuma K, Farkas O, Foresman JB, Fox DJ. *Gaussian 09, Revision E.01.* Wallingford CT: Gaussian, Inc.; 2016.
- Cortopassi WA, Kumar K, Duarte F, Pimentel AS, Paton RS. *J Mol Graph Model.* 2016;67:69.
- McAllister TE, England KS, Hopkinson RJ, Brennan PE, Kawamura A, Schofield CJ. *J Med Chem.* 2016;59:1308.
- Guerra-Calderas L, Gonzalez-Barrios R, Herrera LA, et al. *Cancer Genet.* 2015;208:215.
- Horton JR, Engstrom A, Zoeller EL, et al. *J Biol Chem.* 2016;291:2631.
- Teng YC, Lee CF, Li YS, et al. *Cancer Res.* 2013;73:4711.
- Hu D, Jablonowski C, Cheng PH, et al. *iScience.* 2018;9:84.
- Miyake Y, Itoh Y, Hatanaka A, et al. (in press). *Bioorg Med Chem.* 2019. <https://doi.org/10.1016/j.bmc.2019.02.006>.